THE JOURNAL OF BIOLOGICAL CHEMISTRY
Vol. 275, No. 18, Issue of May 5, pp. 13343–13348, 2000

Printed in U.S.A.

Surface Expression and Single Channel Properties of KCNQ2/KCNQ3, M-type K^+ Channels Involved in Epilepsy*

Received for publication, November 22, 1999, and in revised form, January 28, 2000

Michael Schwake‡§¶, Michael Pusch§‖, Tatjana Kharkovets‡, and Thomas J. Jentsch‡**

From the ‡Zentrum für Molekulare Neurobiologie Hamburg (ZMNH), Universität Hamburg, Martinistrasse 85, D-20246 Hamburg, Germany and the ‖Istituto di Cibernetica e Biofisica, Via de Marini 6, I-16149 Genova, Italy

Mutations in either KCNQ2 or KCNQ3 underlie benign familial neonatal convulsions (BFNC), an inherited epilepsy. The corresponding proteins are co-expressed in broad regions of the brain and associate to heteromeric K^+ channels. These channels mediate M-type currents that regulate neuronal excitability. We investigated the basis for the increase in currents seen after co-expressing these subunits in *Xenopus* oocytes. Noise analysis and single channel recordings revealed a conductance of ≈ 18 pS for KCNQ2 and ≈7 pS for KCNQ3. Different conductance levels (ranging from 8 to 22 pS) were seen upon co-expression. Their weighted average is close to that obtained by noise analysis (16 pS). The open probability of heteromeric channels was not increased significantly. Co-expression of both subunits increased the surface expression of KCNQ2 and KCNQ3 by factors of 5 and >10, respectively. A KCNQ2 mutant associated with BFNC that has a truncated cytoplasmic carboxyl terminus did not reach the surface and failed to stimulate KCNQ3 surface expression. By contrast, several BFNC-associated missense mutations in KCNQ2 or KCNQ3 did not alter their surface expression. Thus, the increase in currents seen upon co-expressing KCNQ2 and KCNQ3 is predominantly due to an increase in surface expression, which is dependent on an intact carboxyl terminus.

Mutations in all four known KCNQ potassium channel genes can cause inherited diseases. Dominant negative mutations in KCNQ1 (also known as KvLQT1) lead to the long QT syndrome, which is characterized by potentially fatal cardiac arrhythmias (1). When mutated on both alleles as in the Jervell and Lange-Nielsen syndrome, patients suffer additionally from congenital deafness (2). Mutations in KCNQ4 lead to DFNA2, a form of dominant, progressive hearing loss (3). Finally, mutations in either KCNQ2 or KCNQ3 lead to benign familial neonatal convulsions (BFNC),[1] a dominantly inherited epilepsy of the newborn (4–6).

KCNQ2 and KCNQ3 are expressed nearly exclusively in the central nervous system (4–6). They are co-expressed in many areas of the brain (7, 8), suggesting that they may form heteromeric potassium channels. This could explain the fact that mutations in either KCNQ2 or KCNQ3 lead to the same clinical phenotype. Indeed, when KCNQ2 and KCNQ3 were co-expressed in *Xenopus* oocytes, currents were much larger than those obtained from KCNQ2 or KCNQ3 alone (7, 9, 10). Additionally, a mutant of KCNQ3 that was constructed in analogy to a dominant negative KCNQ1 mutant suppressed KCNQ2 currents (4), and heteromeric channels showed a decreased sensitivity to the potassium channel blocker tetraethylammonium (10). The pharmacological profile, the voltage dependence, and kinetics of currents suggest that these channels may be a molecular correlate of M-type currents (10). M-type currents, which are exquisitely regulated by several receptor systems (11), are active at the threshold of action potential firing. This renders M-type currents an important regulator of neuronal excitability. All BFNC mutations that have been identified do not exert dominant negative effects, and consequently the reduction of KCNQ2/KCNQ3 currents in patients was predicted to be small (7). Thus, the magnitude of KCNQ2/KCNQ3 currents is probably close to a critical, pathogenic level during early life (7).

Although KCNQ2/KCNQ3 heteromers have typical properties of M-type channels, it seems unlikely that there is just a single M channel. There may be other KCNQ subunits that increase the molecular diversity of M-type currents. For instance, KCNQ4 can form heteromeric channels with KCNQ3. These heteromers display several properties of M-type currents, including a sensitivity to linopirdine (3). Additionally, *eag* (ether-a-gogo)-related channels share some properties with M-type currents (12, 13).

In this study, we investigated the basis for the increase in currents observed upon co-expression of KCNQ2 and KCNQ3 (7, 9, 10). This increase may be due to an increased single channel conductance or open probability, to a larger number of active channels at the cell surface, or to a combination of these factors. We determined the single channel conductances of homo- and heteromeric channels by noise analysis and single channel recordings. Additionally, we determined the surface expression of epitope-tagged channels using a detection system based on luminescence (14). We conclude that the increase in current cannot be explained by an increase in single channel conductance or in open probability but is primarily due to an increased surface expression of active channels. In addition, we identify differential effects on surface expression of KCNQ2 and KCNQ3 mutations that were found in neonatal epilepsy. These results show that the carboxyl terminus is required for an efficient transport to the surface.

EXPERIMENTAL PROCEDURES

Electrophysiology—cRNA synthesis, oocyte injection, and incubation were performed as described (3). cRNA was derived from human KCNQ2 (4) and KCNQ3 (7) cDNAs (or mutants) that had been inserted

* This work was supported by grants from the Deutsche Forschungsgemeinschaft and the Fonds der Chemischen Industrie (to T. J. J.) and by Telethon Italy Grant 1079 (to M. P.). The costs of publication of this article were defrayed in part by the payment of page charges. This article must therefore be hereby marked "*advertisement*" in accordance with 18 U.S.C. Section 1734 solely to indicate this fact.

§ These authors contributed equally to this work.

¶ Ph.D. student of the faculty for biology, chemistry, and pharmacy of the Freie Universität Berlin.

** To whom correspondence should be addressed. Tel.: 49-40-42803-4741; Fax: 49-40-42803-4839; E-mail: Jentsch@plexus.uke.uni-hamburg.de.

[1] The abbreviations used are: BFNC, benign familial neonatal convulsions; HA, hemagglutinin; TBS, Tris-buffered saline; WT, wild type; BSA, bovine serum albumin.

into the oocyte expression vector pTLN (15). Oocytes were injected with 50 nl of cRNA solution. Approximately 5 ng of KCNQ2 or KCNQ3 cRNA or 5 ng of a 1:1 mixture of both were injected per oocyte. For patch clamping, the vitelline layer was removed manually, and the oocytes were then bathed in a solution containing 10 mM KCl, 90 mM potassium glutamate, 2 mM EGTA, 2 mM $MgSO_4$, 5 mM HEPES, pH 7.3. The resting potential of the oocyte in this solution will be close to 0 mV. 2–7 days after injection, recordings were made at 19 ± 1 °C from cell-attached patches. Patch pipettes were made from alumino-silicate glass and were filled with a solution containing 10 mM KCl, 90 mM potassium glutamate, 5 mM $MgSO_4$, 5 mM HEPES, pH 7.3. Currents were recorded with a List EPC-7 amplifier (List, Darmstadt, Germany) and the Pulse program (Heka, Lambrecht/Pfalz, Germany). For noise analysis, data were recorded at 5–10 kHz and low pass filtered at 2–5 kHz. Data were analyzed using self-written software (written in Visual C++, Microsoft) and the SigmaPlot program (Jandel Scientific, Corte Madera). Voltage clamp protocols are described in the figure legends. Leak currents were estimated by assuming that channels are closed completely during a long pulse to −100 mV. Capacity transients were measured from the response to a step to 0 mV (*i.e.* close to the reversal potential) and subtracted off-line. Nonstationary noise analysis was performed as described (16, 17). Statistical errors are given as standard deviations. Two electrode voltage clamping of oocytes was performed using a Turbotec amplifier (npi Instruments, Tamm, Germany) and pCLAMP software (Axon, Foster City, state).

Determination of Surface Expression—To measure surface expression of KCNQ proteins, we used the method recently described by Zerangue *et al.* (14). KCNQ channel subunits were tagged with an HA epitope in the extracellular loop that connects transmembrane domains S1 and S2. To increase the accessibility of the HA epitope by the cognate antibody, we enlarged this short loop (≈9 amino acids) by flanking the epitope with fragments from the extracellular D1-D2 loop of the ClC-5 chloride channel (18) (a similar HA-tagged construct in ClC-5 shows normal channel activity and can be used to measure surface expression).[2] These insertions change the sequence between transmembrane domains S1 and S2 to ^{115}KEYEKSSEG*SEH***YPYDVPDYA***VTFEERD-KCPEWN*A^{126} in KCNQ2 and to ^{145}KEYETVSGD*NSEH***YPYDVP-DYA***VTFEERDKCPEWN*W^{156} in KCNQ3 (HA epitope shown in bold type, and residues derived from ClC-5 are in italics). These mutants were constructed by recombinant polymerase chain reaction and verified by sequencing. Unless otherwise noted, oocytes were injected with 10 ng of cRNA of KCNQ2-HA or KCNQ3-HA or 10 ng of a 1:1 mixture of (*a*) KCNQ2 and KCNQ3 (control), (*b*) KCNQ2-HA and KCNQ3, (*c*) KCNQ3-HA and KCNQ2, or (*d*) combinations with mutants found in epilepsy. After 3 days at 17 °C, oocytes were placed for 30 min in ND96 with 1% BSA at 4 °C to block unspecific binding, incubated for 60 min at 4 °C with 1 μg/ml rat monoclonal anti-HA antibody (3F10 (Roche Molecular Biochemicals) in 1% BSA/ND96), washed at 4 °C, and incubated with horseradish peroxidase-coupled secondary antibody (goat anti-rat FAB fragments, Jackson ImmunoResearch, in 1% BSA for 30–60 min at 4 °C). Oocytes were washed thoroughly (1% BSA at 4 °C for 60 min) and transferred to frog Ringer solution (82.5 mM NaCl, 2 mM KCl, 1 mM $MgCl_2$, 5 mM HEPES, pH 7.5) without BSA. Individual oocytes were placed in 50 μl of Power Signal ELISA solution (Pierce) and incubated at room temperature for 1 min. Chemiluminescence was quantified in a Turner TD-20/20 luminometer (Sunnyvale, CA).

Western Blot Analysis—The oocytes used to measure the surface expression of channel subunits were subsequently pooled and stored at −20 °C. After homogenization of the pooled oocytes in an ice-cold solution containing 250 mM sucrose, 0.5 mM EDTA, 5 mM Tris-HCl (pH 7.4) and a protease inhibitor mix (Complete^R; Roche Molecular Biochemicals), the yolk platelets were removed by three low speed centrifugations. The resulting supernatant was mixed with SDS-Laemmli sample buffer, and the protein equivalent to one oocyte was analyzed by SDS-polyacrylamide gel electrophoresis (8% polyacrylamide). The separated proteins were transferred to nitrocellulose. Blots were blocked in TBS (150 mM NaCl, 25 mM Tris, pH 7.4) containing 5% milk powder and 0.1% Nonidet P-40. Primary (rat anti-HA monoclonal 3F10, 200 ng/ml) and secondary (horseradish peroxidase-conjugated goat anti-rat IgG, 1:10000) antibodies were diluted in TBS blocking solution. Washes were in TBS with 0.1% Nonidet P-40. Reacting proteins were detected by using the Renaissance reagent (NEN Life Science Products) and photographic film (Kodak).

[2] M. Schwake and T. J. Jentsch, unpublished results.

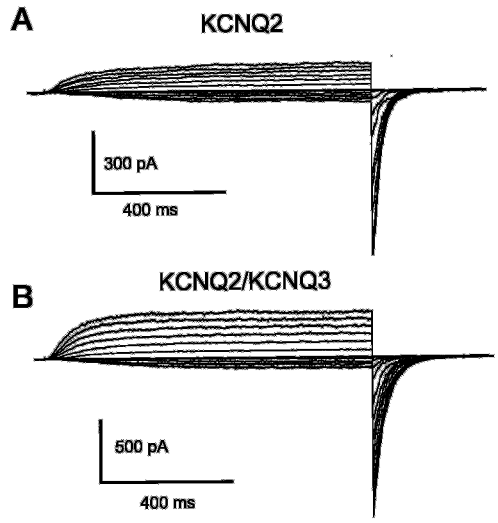

FIG. 1. **Macro-patch recordings of oocytes expressing KCNQ2 (*A*) or co-expressing KCNQ2 and KCNQ3 (*B*).** Voltage clamp traces from cell attached patches are shown. The voltage was clamped from +60 to −70 mV in steps of 10 mV, followed by a fixed tail potential of −100 mV (holding potential, −80 mV; sampling rate, 10 kHz, filtered at 5 kHz).

RESULTS

Two methods were used to measure single channel conductances of homomeric and heteromeric KCNQ2 and KCNQ3 potassium channels. Using noise analysis on macro patches, estimates for single channel conductances were obtained from large ensembles of channels. These values were then corroborated by single channel analysis. This dual approach avoids the problem that single channel recordings may represent channels that do not mediate the bulk of the current.

Noise Analysis—For nonstationary noise analysis, currents of injected oocytes were measured in the cell-attached configuration of the patch-clamp technique. Because of a high potassium concentration in the bath, the resting voltage of the oocytes is expected to be close to 0 mV. The patch pipette also contained a high potassium concentration to increase the inward tail K^+ currents during test pulses to negative voltages. Tail currents were measured after activating the channels by prepulses to positive voltages (+60 mV). Most patches contained several channels, and currents obtained from KCNQ2 and KCNQ2/KCNQ3 expressing oocytes were relatively large (Fig. 1). Smaller currents were obtained for KCNQ3 (*not shown*). Noise analysis was performed by repeatedly applying a depolarizing prepulse followed by the test pulse to −100 mV. At these negative voltages, the channels close, reflecting changes in the open probability (P_{open}). This change in open probability is a prerequisite for performing nonstationary noise analysis. Examples are shown in Fig. 2 for KCNQ2 (Fig. 2*A*), KCNQ3 (Fig. 2*B*), and KCNQ2/KCNQ3 co-expression (Fig. 2*C*). Assuming a reversal potential of 0 mV, the single channel current was converted to conductance by dividing by −100 mV. The average single channel conductances of homomeric KCNQ2 and heteromeric KCNQ2/KCNQ3 channels were practically identical (KCNQ2, 17.8 ± 3.1 pS (n = 8 patches; ± S.D.); KCNQ2/KCNQ3, 16.3 ± 2.5 pS (n = 21)), whereas the conductance of KCNQ3 was about half that value (7.3 ± 0.7 pS (n = 7)) (all values determined at −100 mV). Thus, the large stimulation of macroscopic currents in oocytes co-expressing KCNQ2 and KCNQ3 (7, 10) cannot be explained by an increase in single channel conductance of heteromeric channels. Another possibility is that the maximum open probability of heteromeric channels is increased. From the variance mean plots (Fig. 2), this maximum open probability can be estimated as P_{max} =

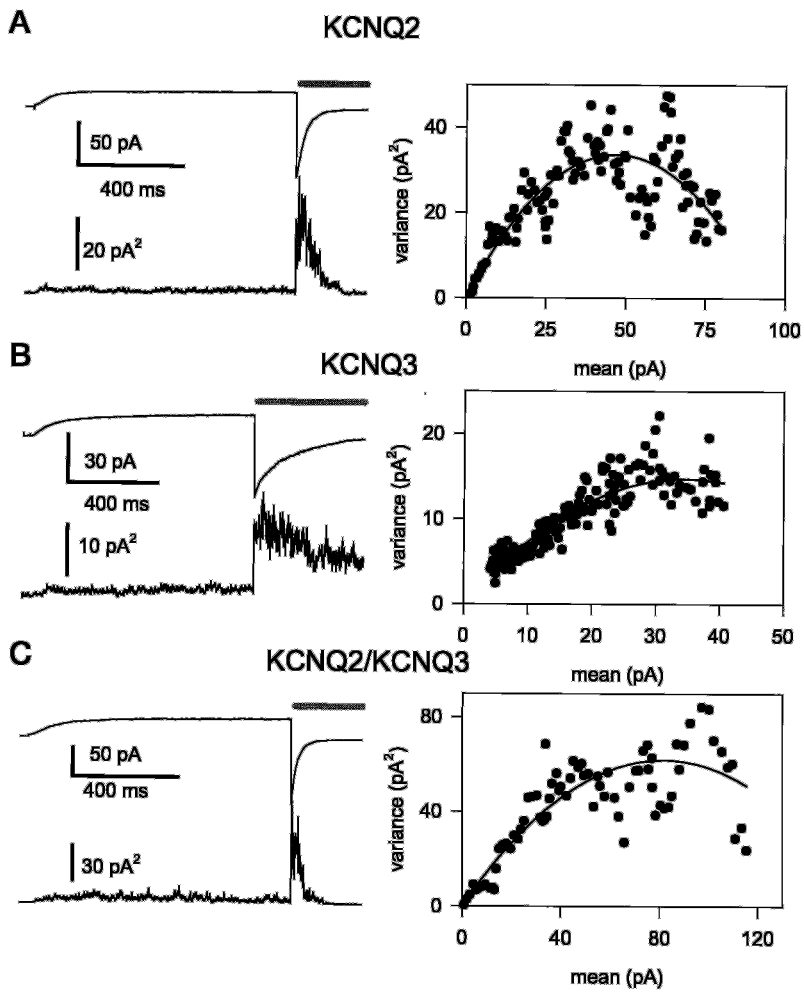

FIG. 2. **Noise analysis of KCNQ2 (*A*), KCNQ3 (*B*), and co-expressed KCNQ2/KCNQ3 (*C*) channels.** The *traces* on the *left side* of each *panel* represent the mean current (*upper trace*) and the variance around the mean (*lower trace*) obtained after repeated voltage steps to +60 mV, followed by the test pulse to −100 mV. These tail currents at −100 mV were used for noise analysis (the interval that was analyzed is indicated by the *bars* above the registrations). On the *right side* of each *panel*, the corresponding variance-mean plots for the test-pulse current are shown, together with fits to the equation $\sigma^2 = i*I - I^2/N$ (where I is the mean current, i is the single channel current, and N is the number of channels (*solid lines*)). For clarity, the current in the variance-mean plot has been scaled by −1. The maximal current corresponds to the start of the deactivating pulse, and thus the initial, maximal open probability that corresponds to the open probability at the end of the depolarizing pre-pulse can be estimated by $P_{max} = I_{max}/N/i$.

$I_{max}/N/i$, where I_{max} is the peak inward current immediately after the voltage step and N and i are the number of channels and the single channel current, respectively. Again the values for homomeric KCNQ2 and heteromeric KCNQ2/KCNQ3 were not significantly different from each other (KCNQ2, 0.61 ± 0.1 (n = 8); KCNQ2/KCNQ3, 0.72 ± 0.1 (n = 21)). The maximal open probability of KCNQ3 was slightly smaller (0.42 ± 0.1 (n = 7)).

Single Channel Recordings—To corroborate the results from our noise analysis, amplitude histograms of single channel events were constructed. Single channels could be observed in patches containing only a few active channels following deactivation of the majority of channels at late time points of the hyperpolarizing test pulse. Examples are shown in Fig. 3. For homomeric KCNQ2 and KCNQ3 channels single channel amplitudes (measured at −100 mV) were quite homogeneous and agreed well with the results from the noise analysis. For KCNQ2, we obtained 18.4 ± 1.5 pS (range, 16.1–20.8 pS; n = 12 patches) (Fig. 3*B*), and for KCNQ3, we obtained 7.4 ± 0.7 pS (range, 6.3–8.6 pS; n = 13 patches) (Fig. 3*C*). In contrast, the current amplitudes of channels obtained from oocytes co-expressing KCNQ2 and KCNQ3 varied from 8 to 22 pS (n = 52 patches) (Fig. 3, *D–F*).This range includes several conductance levels that were not seen with homomeric KCNQ2 and KCNQ3 channels that are expected to be present (albeit with low frequencies) in these co-injection experiments. The weighted mean value of these single channel conductances (16.2 ± 3.7 pS) was similar to the one obtained by noise analysis.

Surface Expression of Wild-type and Mutant Channel Subunits—The large increase in current seen upon co-expressing both subunits in *Xenopus* oocytes (more than 10-fold when compared with homomeric KCNQ2 channels and more than 100-fold when compared with KCNQ3 currents) (7, 10) cannot be explained by a higher single channel conductance or an increased open probability of the heteromeric channels. This leaves the number of active channels at the cell surface as a possible explanation for the increase in current. We therefore investigated whether the amount of KCNQ2 at the surface could be increased by KCNQ3 and *vice versa*. An extracellular HA epitope was inserted into KCNQ2 and KCNQ3 (Fig. 4*A*). Because there are no large extracellular loops in these proteins, it was difficult to choose an insertion site. We opted for the loop between transmembrane domains S1 and S2 to exclude effects on gating or permeation that may result from insertions between S3 and S4 (a determinant of voltage-dependent gating) and between S5 and S6 (which contains the pore loop). However, the small size of the S1/S2 loop of KCNQ2 and KCNQ3 could have impeded the access of the HA antibody (14). To avoid this problem, additional amino acids (16 or 17) were inserted on both sides of the epitope. These amino acids were taken from the large extracellular loop between D1 and D2 of the Cl^- channel ClC-5 (18). This loop was used previously as an insertion site for the HA epitope, leading to functional ClC-5 channels whose surface expression could be monitored with the HA antibody.[2] Expression of these HA-tagged KCNQ constructs in *Xenopus* oocytes led to typical macroscopic currents whose amplitudes, however, were only 50–70% of WT. Thus, these insertions do not change the biophysical properties of the channels but slightly decrease their expression.

The amount of HA epitope at the surface was quantified by

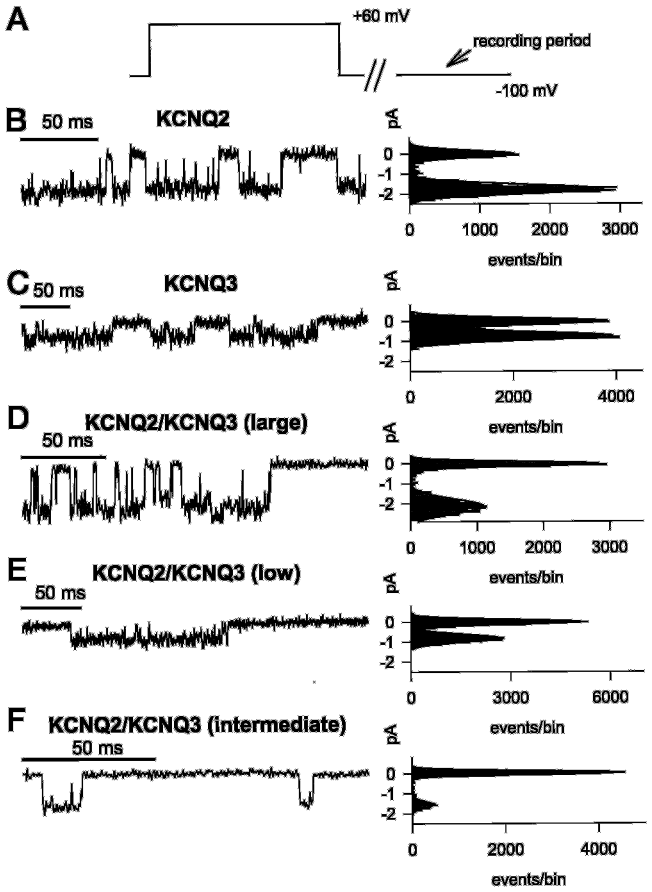

FIG. 3. **Typical single channel traces of KCNQ2 (*B*), KCNQ3 (*C*), and co-expressed KCNQ2/KCNQ3 (*D–F*).** *Traces* on the *left* were recorded during deactivating steps at −100 mV (see *panel A*; the *arrow* indicates the recording period, which began after most channels had deactivated, leaving only one active channel in the membrane patch). *Bars* above the single channel recordings indicate the time scale (50 ms). On the *right side*, amplitude histograms of the traces together with a fit of the sum of two Gaussian functions are shown. The traces for heteromeric KCNQ2/KCNQ3 illustrate the heterogeneity observed for the single channel amplitude. Traces were filtered at 1 kHz. The individual open channel amplitudes for the traces shown are 1.76 pA (*A*), 0.74 pA (*B*), 2.1 pA (*C*), 0.81 pA (*D*), and 1.63 pA (*E*). The current scales apply to both the traces shown on the *left* and to the histograms on the *right*.

incubating nonpermeabilized oocytes with a monoclonal anti-HA antibody. This was followed by an enzymatic amplification procedure that uses chemiluminescence as the final step (14). KCNQ channels devoid of HA epitopes were used as negative controls, and overall protein expression was tested by Western blotting of membranes from the oocytes used for measuring the surface expression. These experiments showed that both KCNQ2 and KCNQ3 reach the surface when injected alone (Fig. 4*B*). The surface expression of KCNQ3 was less than half of that observed for KCNQ2. This low surface expression, together with the lower single channel conductance (≈7 pS *versus* ≈18 pS for KCNQ2) and the lower open probability (≈0.4 *versus* ≈0.6) of KCNQ3, explains that KCNQ3 currents were more than 10-fold lower than those from KCNQ2 (7, 10).

Co-expressing KCNQ2 and KCNQ3 at a 1:1 ratio led to a large increase in surface expression of both KCNQ2 and KCNQ3. The surface expression of KCNQ2 increased by about 4-fold upon co-expression with KCNQ3, likewise that of KCNQ3 increased by more than a factor of 10 (Fig. 4*B*). These findings suggest a major role of increased surface expression in the observed increase in currents upon the formation of heteromers. When KCNQ2 and KCNQ3 were co-expressed, the surface expression of KCNQ2 equaled that of KCNQ3. This is compatible with a 1:1 stoichiometry.

We next investigated the effect of BFNC-associated mutations on surface expression. KCNQ2(1600ins5bp) is a mutation found in an Australian family with BFNC (4). It truncates the KCNQ2 protein in a carboxyl-terminal, cytoplasmic region that is highly conserved between KCNQ channels (Fig. 4*A*). Two other KCNQ2 mutations in BFNC also truncate the protein prior to or within this region (5). When we expressed HA-tagged KCNQ2(1600ins5bp) in *Xenopus* oocytes, we could not detect any significant surface expression (Fig. 4*C*, Q2HA(TR)). Furthermore, this mutant did not enhance the surface expression of KCNQ3 in co-expression experiments. In contrast, KCNQ2 missense mutations in either the pore-forming P-loop (Y284C) or in transmembrane domain S6 (A306T) (5) (Fig. 4*A*) only caused a slight decrease in surface expression, while up-regulating the surface expression of HA-tagged KCNQ3 nearly as much as WT KCNQ2 (Fig. 4*D*). The effects of KCNQ3(G310V), which again changes an amino acid in the P-loop (Fig. 4*A*), did not differ from those of WT KCNQ3 (Fig. 4*E*). G310V is the only KCNQ3 mutation identified so far in BFNC (6). Western blotting demonstrated that the epitope-tagged mutant proteins were produced in similar quantities to the tagged wild-type proteins (Fig. 4, *F* and *G*).

DISCUSSION

KCNQ2 and KCNQ3 subunits assemble to form heteromeric channels that mediate M-type potassium currents (7, 9, 10). In this study, we have determined single channel conductances and open probabilities (P_{open}) of homo- and heteromeric KCNQ2 and KCNQ3 channels. The mean single channel conductance and the open probability of heteromeric channels were not significantly different from those of homomeric KCNQ2 channels, indicating that the increase in currents observed upon co-expressing both subunits in *Xenopus* oocytes cannot be explained by an increase in these parameters. Single channel recordings of *Xenopus* oocytes co-injected with both subunits revealed various single channel conductances, which probably reflect homomeric channels and heteromeric channels with different subunit stoichiometries. However, the present experiments do not allow us to correlate single channels with heteromeric channels of defined composition.

Measurements of surface expression of epitope-tagged homo- and heteromeric channels revealed that both subunits traffic much more efficiently to the surface when they are co-expressed. Thus an increased surface expression is the main factor leading to larger macroscopic currents upon co-expression. The roughly 4-fold increase in surface expression of KCNQ2HA upon co-expression with KCNQ3 suggests an 8-fold increase in channels at the surface, because homomeric KCNQ2HA channels have four tagged subunits, whereas on average heteromeric KCNQ2HA/KCNQ3 channels are likely to have only two tagged subunits. This assumption is supported by data suggesting that either KCNQ2HA or KCNQ3HA, upon expression with the respective untagged partner, display a similar degree of surface expression, which is compatible with an overall 2:2 stoichiometry of heteromeric channels (which almost certainly will form tetramers). The roughly 8-fold increase in the number of channels at the surface compares well with the observed (7) 10- to 15-fold increase in current observed upon co-expression under identical experimental conditions. Because the total amount of cRNA injected in all experiments remained constant, problems associated with a saturation of the expression machinery of oocytes were minimized. One factor that might account for the remaining difference between the increase in surface expression and the increase in current could be the insertion of the HA epitope, which decreased

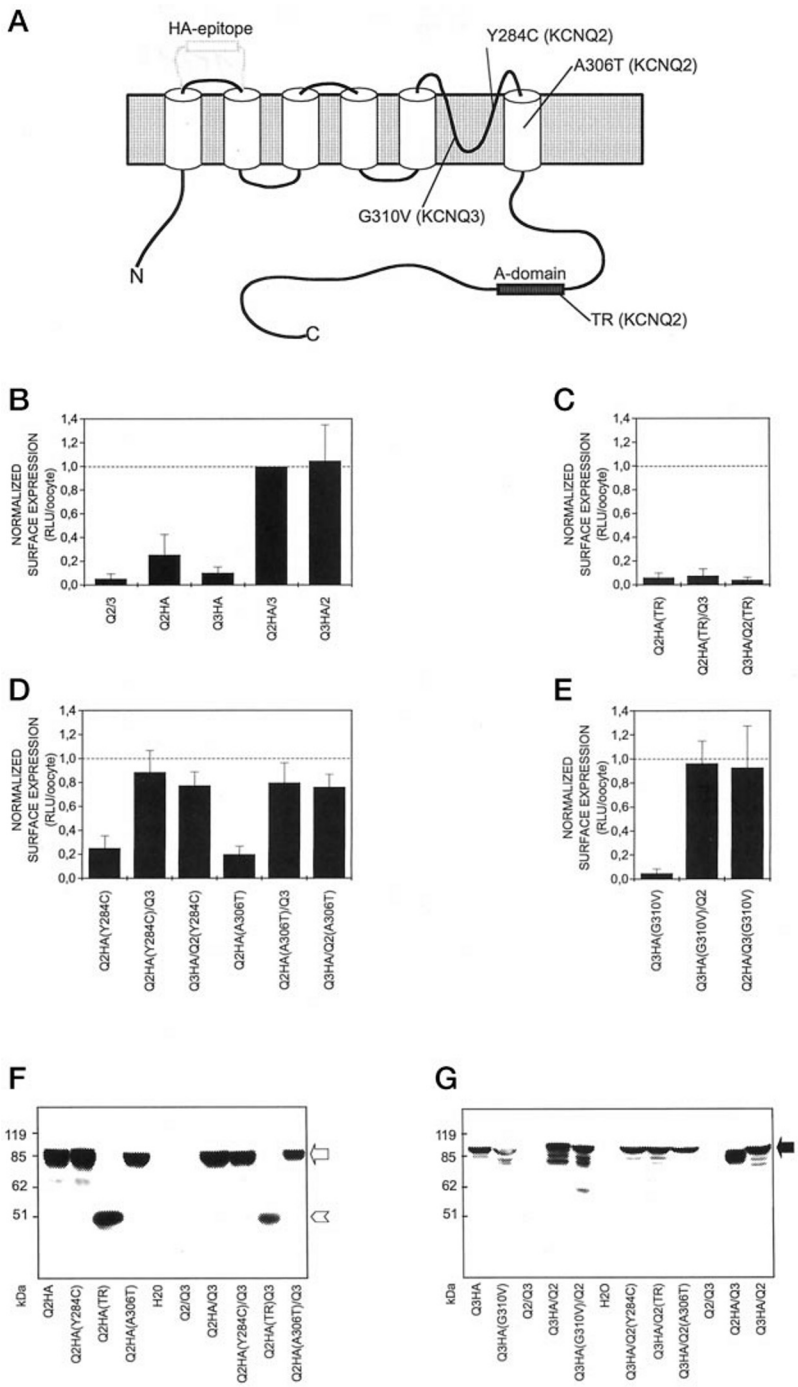

FIG. 4. **Surface expression of KCNQ2, KCNQ3, and some of its mutants found in neonatal epilepsy.** *A*, topological model of KCNQ channels showing the site of insertion of the HA epitope (used to measure surface expression (14), see "Experimental Procedures") and the BFNC mutants analyzed in this work. Two of these mutants (G310V (6) and Y284C (5)) change residues in the pore-forming P-loop, A306T (5) affects a residue in the sixth transmembrane domain, whereas an insertion of 5 base pairs at position 1600 leads to a truncation (labeled *TR*) (4) of the channel at the beginning of the conserved cytoplasmic A domain. *B*, surface expression of epitope-tagged wild-type KCNQ2 and KCNQ3 (labeled Q2HA and Q3HA, respectively). Oocytes co-injected with KCNQ2 and KCNQ3 not containing the epitope (Q2/Q3) serve as a negative control. Q2HA is expressed at the surface, as is Q3HA, albeit at lower levels. Co-injection of both subunits leads to a large increase in surface expression for both Q2HA and Q3HA. *C*, surface expression of a tagged carboxyl-terminal deletion mutant (KCNQ2(1600ins5bp) (4). Q2HA(TR)) was not significantly different from negative controls (Q2/3, *panel B*) and did not stimulate the surface expression of tagged KCNQ3 (Q3HA and Q3HA/Q2(TR)). Also its surface expression was not stimulated by co-expression with Q3 (compare Q2HA(TR) with Q2HA(TR)/Q3). By contrast, in *D* the BFNC mutants Q2HA(Y284C) and Q2HA(A306T) reached the surface nearly as efficiently as Q2HA and stimulated the surface expression of KCNQ3. Further, their own surface expression was stimulated by KCNQ3. *E*, the only known BFNC mutant in KCNQ3, G310V, reached the surface as efficiently as WT and had a similar stimulatory effect on Q2 expression. Columns represent averages from three batches of oocytes, with 5–10 oocytes/batch. Values are normalized to the surface expression of Q2HA/Q3, which was measured with each batch. *Error bars* represent standard deviations. *F* and *G*, Western blot analysis of protein expression from epitope-tagged KCNQ2 and KCNQ3 subunits, respectively. The oocytes that were used for the experiments shown in *B–E* were pooled and assayed for the overall expression of HA-tagged subunits using the antibody directed against the HA epitope. The *arrow* in *F* denotes the molecular weight of HA-tagged KCNQ2 proteins, and the *arrowhead* below that represents the weight of the truncated HA-tagged KCNQ2 protein. The *arrow* in *G* indicates HA-tagged KCNQ3. HA-tagged KCNQ2 (*second lane* from the *right*) migrates slightly faster. Note that overall a constant total amount of cRNA has been injected; thus, oocytes co-expressing a tagged and a nontagged subunit have obtained only half the moles of tagged cRNA.

currents to 50–70% of wild type.

M channels in native tissues have a reported single channel conductance of 7–11 pS in rat sympathetic neurons (19–21) and cultured CA1-CA3 pyramidal neurons (22). These values agree well with our estimates for heteromeric KCNQ2/KCNQ3 and homomeric KCNQ2 if one considers that the native channels were recorded under asymmetric, low extracellular K conditions. In the asymmetric solutions the slope conductance is expected to be reduced by a factor of about 1.5 at 0 mV when compared with symmetrical solutions because of the Goldman rectification (23). In addition, the heterologously expressed channels displayed a slight instantaneous inward rectification even under symmetrical potassium concentrations.

Our analysis shows that mutants with a truncated carboxyl terminus do not reach the surface. In contrast, we demonstrate that channels having missense mutations in the transmembrane block (S1–S6) can assemble to form homo- and heteromeric channels that are nearly as efficiently expressed at the plasma membrane as WT channels. These results agree with previous electrophysiological analyses. Currents from KCNQ2-(Y284C) homomeric channels were 30–60% of WT currents (7). In the absence of a difference in surface expression, this suggested that the channel functions less efficiently. In contrast, the carboxyl-terminal truncation mutant KCNQ2(1600ins5bp) did not yield detectable currents (4). However, it is beyond the scope of the present work to investigate whether the reduced currents (7) of these missense mutations identified in BFNC are due to a decrease in P_{open} or in single channel conductance.

The lack of surface expression of the truncated subunit is compatible with the notion that the carboxyl terminus is required for the association of these subunits to form homo- or heteromeric channels, which in turn is necessary for reaching the surface. Indeed, the carboxyl termini of all known KCNQ proteins contain a highly conserved domain (which we propose to name the "A domain") (Fig. 4*A*). It is tempting to speculate that the A domain is involved in subunit interactions. This would also explain why a similar truncation in KCNQ1 found in the recessive Jervell and Lange-Nielsen syndrome (2) does not lead to a dominant negative effect (24). However, additional experiments are required to test this hypothesis.

Many ion channels are heteromers of homologous pore-forming subunits or other associated nonhomologous subunits. In many cases only the correctly assembled channels reach their target membranes. For instance, although the α-subunit of the epithelial Na^+ channel yields some currents (25), these are greatly enhanced by co-expressing the homologous β and γ subunits (26). This is primarily due to an increase in surface expression (27). The ATP-regulated potassium channel K_{ATP} is composed of four Kir6.1 (or Kir6.2) subunits and four sulfonylurea receptor subunits. Both types of subunits are necessary for current expression. Again, co-expression of both subunits is necessary for trafficking to the surface (14). A novel endoplasmic reticulum retention motif (RKR) was identified in the carboxyl termini of each subunit and is apparently masked by the complementary subunit. This leads to an endoplasmic reticulum quality control mechanism that ensures that only correctly assembled channels reach their final destination (14). Likewise, KCNQ proteins, including KCNQ2 and KCNQ3, have another cluster of positively charged amino acids (KRK) at the beginning of the A domain. However, extensive mutagenesis of the Kir6.2 retention signal (14) suggests that this tripeptide will not serve as an endoplasmic reticulum retention signal. Furthermore, the requirement for the complementary subunit is not as strict as with K_{ATP}.

In summary, our data show that the increase in current seen upon co-expression of KCNQ2 and KCNQ3 cannot be explained by an increase in single channel conductance or in the open probability of heteromeric channels. Rather, it is due to a more efficient surface expression of heteromers. These heteromers may have different stoichiometries as suggested by our single channel analysis. Differing stoichiometries may increase further the molecular diversity of M-type currents and may have implications for those forms of epilepsy that are due to mutations in KCNQ2 and KCNQ3.

Acknowledgments—We thank B. Schwappach for communicating the novel surface labeling procedure prior to publication, L. Bertorello for excellent technical assistance, and John E. Cuffe and Heather Ostendorff for critical reading of the manuscript.

REFERENCES

1. Wang, Q., Curran, M. E., Splawski, I., Burn, T. C., Millholland, J. M., VanRaay, T. J., Shen, J., Timothy, K. W., Vincent, G. M., de Jager, T., Schwartz, P. J., Toubin, J. A., Moss, A. J., Atkinson, D. L., Landes, G. M., Connors, T. D., and Keating, M. T. (1996) *Nat. Genet.* **12,** 17–23
2. Neyroud, N., Tesson, F., Denjoy, I., Leibovici, M., Donger, C., Barhanin, J., Faure, S., Gary, F., Coumel, P., Petit, C., Schwartz, K., and Guicheney, P. (1997) *Nat. Genet.* **15,** 186–189
3. Kubisch, C., Schroeder, B. C., Friedrich, T., Lütjohann, B., El-Amraoui, A., Marlin, S., Petit, C., and Jentsch, T. J. (1999) *Cell* **96,** 437–446
4. Biervert, C., Schroeder, B. C., Kubisch, C., Berkovic, S. F., Propping, P., Jentsch, T. J., and Steinlein, O. K. (1998) *Science* **279,** 403–406
5. Singh, N. A., Charlier, C., Stauffer, D., DuPont, B. R., Leach, R. J., Melis, R., Ronen, G. M., Bjerre, I., Quattlebaum, T., Murphy, J. V., McHarg, M. L., Gagnon, D., Rosales, T. O., Peiffer, A., Anderson, V. E., and Leppert, M. (1998) *Nat. Genet.* **18,** 25–29
6. Charlier, C., Singh, N. A., Ryan, S. G., Lewis, T. B., Reus, B. E., Leach, R. J., and Leppert, M. (1998) *Nat. Genet.* **18,** 53–55
7. Schroeder, B. C., Kubisch, C., Stein, V., and Jentsch, T. J. (1998) *Nature* **396,** 687–690
8. Tinel, N., Lauritzen, I., Chouabe, C., Lazdunski, M., and Borsotto, M. (1998) *FEBS Lett.***438,** 171–176
9. Yang, W.-P., Levesque, P. C., Little, W. A., Conder, M. L., Ramakrishnan, P., Neubauer, M. G., and Blanar, M. A. (1998) *J. Biol. Chem.* **273,** 19419–19423
10. Wang, H. S., Pan, Z., Shi, W., Brown, B. S., Wymore, R. S., Cohen, I. S., Dixon, J. E., and McKinnon, D. (1998) *Science* **282,** 1890–1893
11. Marrion, N. V. (1997) *Annu. Rev. Physiol.* **59,** 483–504
12. Selyanko, A. A., Hadley, J. K., Wood, I. C., Abogadie, F. C., Delmas, P., Buckley, N. J., London, B., and Brown, D. A. (1999) *J. Neurosci.* **19,** 7742–7756
13. Meves, H., Schwarz, J. R., and Wulfsen, I. (1999) *Br. J. Pharmacol.* **127,** 1213–1223
14. Zerangue, N., Schwappach, B., Jan, Y. N., and Jan, L. Y. (1999) *Neuron* **22,** 537–548
15. Lorenz, C., Pusch, M., and Jentsch, T. J. (1996) *Proc. Natl. Acad. Sci. U. S. A.* **93,** 13362–13366
16. Pusch, M. (1998) *Pflügers Arch.* **437,** 172–174
17. Pusch, M., Steinmeyer, K., and Jentsch, T. J. (1994) *Biophys. J.* **66,** 149–152
18. Steinmeyer, K., Schwappach, B., Bens, M., Vandewalle, A., and Jentsch, T. J. (1995) *J. Biol. Chem.* **270,** 31172–31177
19. Selyanko, A. A., Stansfeld, C. E., and Brown, D. A. (1992) *Proc. R. Soc. Lond. B Biol. Sci.* **250,** 119–125
20. Selyanko, A. A., and Brown, D. A. (1993) *J. Physiol. (Lond.)* **472,** 711–724
21. Selyanko, A. A., and Brown, D. A. (1996) *Neuron* **16,** 151–162
22. Selyanko, A. A., and Sim, J. A. (1998) *J. Physiol. (Lond.)* **510,** 71–91
23. Goldman, D. E. (1943) *J. Gen. Physiol.* **27,** 37–60
24. Wollnik, B., Schroeder, B. C., Kubisch, C., Esperer, H. D., Wieacker, P., and Jentsch, T. J. (1997) *Hum. Mol. Genet.* **6,** 1943–1949
25. Canessa, C. M., Horisberger, J. D., and Rossier, B. C. (1993) *Nature* **361,** 467–470
26. Canessa, C. M., Schild, L., Buell, G., Thorens, B., Gautschi, I., Horisberger, J. D., and Rossier, B. C. (1994) *Nature* **367,** 463–467
27. Firsov, D., Schild, L., Gautschi, I., Merillat, A. M., Schneeberger, E., and Rossier, B. C. (1996) *Proc. Natl. Acad. Sci. U. S. A.* **93,** 15370–15375